Journal of Operation and Automation in Power Engineering

vol. 12, no. 4, Dec. 2024, Pages: 365-378

http://joape.uma.ac.ir

Enhancement in Voltage Stability Using FACTS Devices Under Contingency Conditions

*S.K. Gupta**, *S.K. Mallik*

Department of Electrical Engineering, National Institute of Technology, Patna, Bihar, India

Abstract— *The voltage stability margin (VSM) is an important indicator to access the voltage stability of the power system. In this paper, Flexible AC transmission systems (FACTS) devices like static synchronous compensator (STATCOM), static synchronous series compensator (SSSC), and unified power flow controller (UPFC) have been deployed to enhance the VSM of the power system. The placement of the FACTS devices is decided based on contingency raking. For the top five critical contingencies, the most severe bus is selected based on bus voltage stability criticality index and degree centrality methods. The critical line is decided based on the values of the line stability index, fast voltage stability index, and line stability factor. The STATCOM and shunt part of the UPFC are placed at the critical bus, whereas the SSSC and series part of the UPFC are placed at the critical line for enhancing voltage stability. The proposed method for voltage stability enhancement using FACTS devices is tested and validated on the IEEE-14 bus system and the NRPG-246 bus system at different system loading scenarios. The impact of the placement of FACTS devices is validated in terms of VSM improvement.*

Keywords—Contingency, FACTS, Indices, Voltage Collapse, VSM.

NOMENCLATURE

Terminology	Description
STATCOM	Static synchronous compensator
VC	Voltage collapse
Lqp	Line stability factor
Lmn	Line stability index
CBI	Critical boundary index
NRPG	Northern region power grid
$P_{D_{ib}}$	Maximum real power demand limit at bus 'i'
VSM	Voltage stability margin
CPF	Continuation power flow
FVSI	Fast Voltage Stability Index
P_i	Sending end real power flow
BVSI	Bus voltage stability criticality index
SSSC	Static synchronous series compensator
Cd	Degree centrality
θ_{ij}	Line impedance angle between bus 'i' and 'j'
$Q_{D_{ib}}$	Maximum reactive power demand limit at bus 'i'
Q_i	Sending end reactive power flow
λ	Loading factor
$\lambda_{\max}$	Maximum loading factor
k	Loading multiplier
X_{ij}	Line reactance bus 'i' and 'j'
Q_j	Receiving end reactive power flow
P_j	Receiving end real power flow
δ	Power angle
y_{ij}	Line admittance between bus 'i' and 'j'
LO	Line Outage
R	Ranking
UPFC	Unified power flow controller

Received: 23 Sep. 2022
Revised: 18 Feb. 2023
Accepted: 08 Jun. 2023
*Corresponding author:
E-mail: santoshg.phd19.ee@nitp.ac.in (S.K. Gupta)
DOI: 10.22098/joape.2023.11569.1864
Research Paper

1. INTRODUCTION

An increase in linear and non-linear loads due to technological development, restructuring, increasing interconnection, environmental, and economic factors are responsible for susceptible and more complex power systems operating near their stability limit [1]. The primary purpose of the restructured power system is to lower power loss and investment and to maximize the utilization of power system networks [2]. The sources of disturbances are increased due to deregulated power systems which result in unpredictable and less robustness of systems [3]. Long-term stability doesn't have assured short-term stability. Consequently, many blackouts have been reported all over the world in the last decade due to voltage instability problems [4]. The voltage instability is referred to the uncontrolled voltage drop of the transmission system, which may lead to disruption of the system. The voltage instability problem arises when the power system operates beyond its generation and transmission capability. The progressive drop in voltage magnitude, which leads to the blackout of a significant part of the power system network, is known as voltage collapse (VC). The event of voltage collapse includes sudden loss of generators, overloading of the transmission line, sudden significant disturbance, or minor continuous disturbances [5, 6]. Generator exciter and overload tap changers restore the voltage quickly in the power system network. Tap changing operation results in an increase in load, which will increase the line losses. Further, this will increase the voltage drop in load level. As result, the reactive power output of the generator will reach its excitation limit. Further additional reactive power will be managed by generators nearest in resulting overloading of several generators. The successive outages of generators and transmission lines would lead to a complete blackout [7].

It is very essential to know the margin of the power system stability to avoid and prevent voltage collapse or blackout. The concept of voltage stability index was developed to find out how the power system is near its stability limit (voltage collapse point). These indices values would precisely indicate system state

as variations in system parameters. In [8], the first developed voltage stability index to determine the voltage instability based on Jacobian. Several methods have been developed for the assessment of voltage stability, like modal analysis, eigenvalue, singular value, and sensitivity methods [9, 10]. For static and dynamic loads, a novel index based on V-Q sensitivity is proposed [11]. The reactive powers sensitivity matrix of the generators can be quickly established for the loading parameter. The high value of the sensitivity factor indicates critical loads and critical generating units. The indices based on Jacobian have drawbacks as they are required high computation and high accuracy for online applications. Voltage stability margin (VSM) is the more accurate and widely accepted method for predicting voltage collapse [12]. It is measured by direct method or continuation power flow (CPF) and used for a dynamic system with consideration of parameter limits and nonlinearity. Some voltage stability indices have been developed based on online parameters (line admittance/impedance) and variables like power flow, bus voltages as well as line current. Further, these indices are categorized into bus voltage stability indices and line voltage stability indices [13]. Several advantages of finding the critical lines over detecting the critical bus in the power system network using indices have been discussed in [14]. Using Thevenin's equivalent impedance matching technique have been proposed to determine the voltage stability limits in [15]. However, it is seen that by taking into account the variation of active and reactive powers at the same instant, the voltage stability analysis provides high accuracy. In this situation, the critical boundary index (CBI) has been used to measure the physical distance from the operating point to the point close to voltage collapse (known as voltage stability margin) [16].

A hybrid approach was developed by the author in [17] to access the voltage stability based on PMU measurement with considering generator's reactive power reserve limits. For the monitoring of the wide area, a fast voltage stability index was developed [18]. A novel voltage stability assessment algorithm (VSAA) is evaluated from power flow equations in [19] and it is validated under different loading, different generator outages, and load disturbances. A new global voltage stability index (VRI_{sys}) was formulated to access the short-term voltage stability in [20]. A new line voltage stability index (BVSI) was formulated for finding the most severe line of the power system, which was tested under, heavy reactive power loading, heavy active power loading, heavy apparent power loading, (N-1) contingencies [21]. It is possible to represent an electrical network by the graph. The centrality measures can rank the relative importance of the nodes and edges in a network graph [22]. Like graph theory, the concept of degree centrality has been used in grid networks by considering electrical parameters to identify the most critical bus of the network [23]. The enhancement of reactive power to improve the voltage profile and voltage stability margin is based on contingency ranking. The contingency ranking can be based on the voltage stability margin, performance index, loadability of the power system, and the voltage level of the buses. The requirement of reactive power compensation can be met by rescheduling the generators, changing the tap of the transformers, load shedding, and providing external reactive power support.

Contingencies can be ranked based on the line stability index [24]. The appropriate buses of the system for DGs placement can be decided by analytical approaches using the loss sensitivity factor [25]. The voltage stability analysis has been evaluated under unbalance conditions using distributed generation sources [26]. Several control techniques have been employed in the power system, such as reactive power compensation devices (shunt capacitor, Flexible AC Transmission System, synchronous condenser, etc.), load shedding, tap changing transformer with proper adjustment, et cetera can overcome the voltage instability and voltage collapse problems [27]. The power flow of any electrical network can be easily controlled by regulating the line parameters, magnitude, and phase angle of the bus voltages. The concept of a novel Flexible AC Transmission System (FACTS) was proposed in [28] to regulate these parameters at the power system level. Since then, to improve the power handling capability of the line and power system stability, the allocation of FACTS devices in the network has become a wide area of interest for researchers and operators. Genetic algorithms, particle swarm optimization, L-index, sensitivity-based approaches, and modal analysis are the vast areas used for the optimal allocation of FACTS [29]. The area of the voltage stability region has been visualized in [30]. The improvement of the VSM has been investigated using PMUs at the appropriate locations [31]. In [32], the FACTS devices SVC and TCSC were placed at optimal locations at minimum investment cost. The optimal location of SVC and TCSC are found as bus number 10 and line (9-14) for the IEEE-14 bus system. Line outage (6-13) contingency is found as the most important contingency. In [33], the voltage stability margin is improved by five different FACTS devices. The most critical line and bus are found as line (1-5) and bus 14 for the IEEE-14 bus system by reactive power loss sensitivity approach and tangent vector analysis respectively. The most severe contingency is found as the line outage (2-3) for IEEE-14 bus system. The maximum voltage stability margin is obtained when UPFC is placed in the system. In [34], the voltage stability margin was improved by minimizing the voltage stability index Lmax. A Multi-Objective Genetic Algorithm (MOGA) was used to minimize Lmax and the Investment cost of the SVC and TCSC FACTS devices by keeping a minimum deviation of the generator's real power. The voltage stability has been accessed by increasing the Doubly-Fed Induction Generator-based (DFIG)-based Wind Energy Conversion System (WECS) power penetration in [35]. In this, the effects of increasing the DFIG-based WECS power penetration on generator loading, transformer loading, and on transmission line loading have been analyzed.

This paper presents a simple method to improve the voltage stability margin using series and shunt FACTS devices with wide variations in Q_D/P_D. Q_D and P_D are the reactive and real power demands at buses. A system load multiplier k is considered to vary Q_D/P_D, which gives wide variations in load patterns. Load flow analysis data has been used to calculate the voltage stability indices and identify the voltage stability boundary. This work is mainly focused on a comparative analysis of the effects of FACTS devices, such as STATCOM, SSSC, and UPFC on the voltage stability margin or loadability of the load buses using continuation power flow (CPF). Based on VSM critical contingencies have been determined. The most severe contingency is that which has lower a VSM. Critical boundary index (CBI) and degree centrality measures methods have been employed to find out the critical bus and for the placement of the shunt FACTS device STATCOM. While for the placement of series FACTS devices SSSC and series part of the UPFC, the fast voltage stability index (FVSI), line stability index (Lmn), and line stability index (Lqp) methods are used to determine the most critical line. The proposed method with the placement of the FACTS device has also been investigated with the deployment of the DFIG-WECS.

The proposed work has mainly the following highlights:

- Critical contingencies ranking has been to identify the most critical contingencies with wide variations in load.
- The locations of shunt and series FACTS controllers have been identified using bus voltage stability indices and line voltage stability indices respectively.
- Enhancement of loadability of the load bus or VSM with shunt and series FACTS device and their comparative study.

2. VOLTAGE STABILITY MARGIN (VSM)

The transmission line has a limited capacity for carrying both active and reactive power. The network's voltage stability is impacted by this power system limitation. The sustainability of voltages on each bus in the power system within a reasonable range is referred to as the voltage stability of a system.

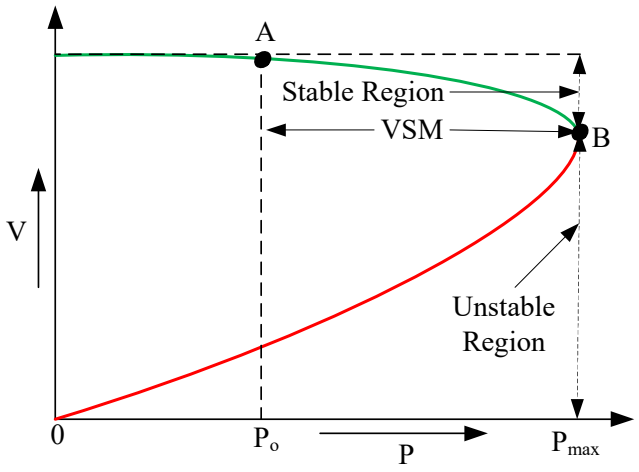

Fig. 1. P-V Curve of a power system

Due to the increase in power demand, the voltage magnitude decreases. The decrease in voltage magnitude will lead to an increase in power till the point of voltage collapse, "B". Beyond this point, there is no increase in power even after the decrease in voltage. It will lead to voltage collapse. In Figure 1, the region beyond point B is unstable and is denoted in red color. The system should operate in the stable area indicated by the green color. The stability of the system is evaluated in terms of VSM. The distance between the operating point, A, and the nose point, B, is known as the VSM. VSM is considered to be an indicator of the voltage stability of the power system [36]. Increasing the distance between the operating point and the nose point will improve the VSM. This can be achieved by either lowering the operating point or increasing the nose point. The operating point can be reduced by reducing the system loading, which is not a feasible solution to improve the VSM [37]. The nose point can be shifted right by providing additional reactive power support in the system.

3. CONTINGENCY RANKING

On increasing the system loading, the operating point is shifted right (refer to Figure 1) and hence, the VSM of the power system is reduced. To improve the voltage stability of the power system, reactive power support at a suitable bus is needed. The selection of a suitable bus is decided by CPF [38].

Apart from the different system loading conditions, the VSM of the power system is also affected under different contingency conditions. In this paper, the (N-1) line outage contingencies for base case loading conditions are considered to rank the contingencies under normal operating scenarios. Under contingency, the operating point, as well as the nose point both, will change and hence the voltage stability of the system will degrade. To improve the VSM, reactive power support is needed at the critical bus. The gap between the maximum loadability point and the operating point of the base case with a single line outage at a time has been used to rank contingencies in order to identify the critical bus. The most severe contingency is who has the lowest VSM.

3.1. Contingency Under Different System Loading Conditions

For a given system network condition, the maximum loading point is estimated using CPF. In this paper, branch outages have been considered as contingency conditions. For each line outage, the network condition may change and hence, the maximum loading of the system will also change. For a given line outage,

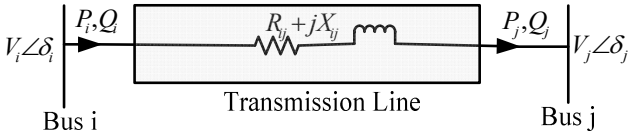

Fig. 2. Block diagram of two bus power systems

the VSM will be assessed with wide variations of real and reactive power demands at the load buses [38]:

$$P_{D_i} = P_{D_{ib}}(1+\lambda) \tag{1}$$

$$Q_{D_i} = kQ_{D_{ib}}(1+\lambda) \tag{2}$$

where $P_{D_{ib}}$ and $Q_{D_{ib}}$ are the real and reactive power demand at *i*th bus respectively at base case; P_{D_i} and Q_{D_i} are the real and reactive power demand at the *i*th bus; the system loading factor known as $\lambda_{\max}$ applies to all buses. Using the system loading factor (multiplier k), the system Q_D/P_D ratio can be varied. The value of multiplier k is chosen as 0.2, 0.5, 1.0, and 1.2 which would give a large deviation in Q_D/P_D. Similarly, the system loading factor $\lambda_{\max}$ may be evaluated for all line outage contingencies. Then, $\lambda_{\max}$ is used to order each contingency and find the critical contingency. The critical contingencies are decided based on the lowest system loading factor and computed for all values of k.

Severe critical contingencies cases for all values of k are most sensitive toward the voltage instability and are required for further analysis. The reactive power support technique is the most potent method to enhance the power transfer capability of the line and improve the VSM and voltage level of the buses. By controlling the injection and absorption of reactive power, the bus voltage level can be controlled. This can be accomplished using series and shunt FACTS devices at appropriate locations in the power system. The series and shunt FACTS devices in the power system are placed at the appropriate line/bus using the most critical line/bus under critical contingency.

3.2. Location of Shunt FACTS Devices

Shunt FACTS devices are placed at the most severe bus of the system. Bus voltage stability criticality index (BVSI) [16] and degree centrality (Cd) [22] methods have been employed to identify the most severe bus of the systems.

A) Bus Voltage Stability Criticality Index (BVSI)

For a given two-bus system between bus *i* and *j*, as shown in Fig. 2, the critical boundary index (CBI) is defined as:

$$CBI_{ij} = \sqrt{\Delta P_{ij}^2 + \Delta Q_{ij}^2} \tag{3}$$

where the distances between the operating point and nose point (defined by $\lambda_{\max}$) of the real and reactive power, respectively, are ΔP_{ij} and ΔQ_{ij}. Hence, the expression of BVSI for the *i*th bus can be written as:

$$BVSI(i) = \frac{\sum_j |CBI_{ij}|}{n-1}, \qquad (i \neq j) \tag{4}$$

where n represents the overall system bus count. With the increased value of BVSI, the bus voltage stability will improve.

B) Degree Centrality

The most simple and direct centrality for any vertex is node degree. The degree of a node's centrality determines how connected that node is to the other nodes in the network. For any node v in a network with a graph $G = (V, E)$ with n vertices, a set of

vertices denoted by V, and a set of edges denoted by E, the degree centrality is denoted by [22]:

$$C_d(v) = \frac{\deg(v)}{n-1} = \frac{L(v,v)}{n-1} \tag{5}$$

where L represents Laplacian, and $n-1$ is used for normalization. In an electrical power system network, the connectivity strength of any node (bus) with the connected links is dependent upon the admittance of links (lines). Hence, electrical degree centrality is defined by:

$$C_d(i) = \frac{\sum_j |y_{ij}|}{n-1}, \qquad (i \neq j) \tag{6}$$

where y_{ij} is the admittance of the line connected between bus *i* and *j*. The node having electrical degree centrality near zero is the most severe bus and the node having electrical degree centrality near 1 is the most stable bus.

3.3. Location of Series FACTS Devices

The series FACTS devices should be placed at the most critical line under critical contingency conditions. To select the most critical lines of the system, a number of indices have been developed by power system researchers based on load flow analysis. In this paper, three indices have been discussed for selecting the critical line.

A) Line stability index

The line stability index, L_{mn} has been frequently used by researchers to define the stability criterion of each line [39]. It is expressed as:

$$L_{mn} = \frac{4X_{ij}Q_j}{(V_i \sin(\theta_{ij} - \delta))^2} \tag{7}$$

where, X_{ij} and θ_{ij} are the line reactance and line impedance angle between bus *i* and bus *j*, respectively; Q_j and V_i are the receiving end reactive power and sending end bus voltage magnitude, respectively; $\delta = \delta_i - \delta_j$ for two bus systems shown in Fig. 2.

B) Fast Voltage Stability Index (FVSI)

FVSI of a line is also used to select the critical line and is mathematically defined as [13]:

$$FVSI = \frac{4\,|Z_{ij}|^2\, Q_j}{V_i X_{ij}} \tag{8}$$

where Z_{ij} is the line impedance between bus *i* and bus *j*.

C) Line Stability Factor (Lqp)

The line stability factor is also used for finding the critical line and defined in terms of real and reactive power as [14]:

$$Lqp = 4\left(\frac{X_{ij}}{{V_i}^2}\right)\left(\frac{X_{ij}}{{V_i}^2}{P_i}^2 + Q_j\right) \tag{9}$$

where P_i is the active power at sending end of the line. The lqp value of the system should be less than 1 for the stable and secure operation of a system. The stable condition of the system is decided by an index, Lmn/FVSI/Lqp.

3.4. FACTS Devices for Improvement of VSM

In this paper, STATCOM, SSSC, and UPFC FACTS devices are deployed in the power system network on a critical bus/line. With the deployment of these devices, stability enhancement has been investigated.

A) STATCOM

The STACOM is the most potent FACTS device, which is connected in shunt with the AC load buses. The STATCOM can regulate bus voltages by injecting reactive power at the buses based on bus voltage reference values.

B) SSSC

In order to make up for the reactive and resistive voltage drops, the SSSC is connected in series with a line and is capable of transferring both active and reactive power.

C) UPFC

UPFC is the fast-acting reactive power compensating device within the family of FACTS devices. It has a powerful ability to control all the regulating parameters of the system like line impedance, bus voltages magnitude as well power angle. The UPFC is the combination of two (series and shunt types) FACTS devices. One is STATCOM connected in shunt with the line, and the other is SSSC connected in series with the line, and both are linked with a common dc capacitor for reactive power exchange between them. As UPFC controls all the system parameters, the active and reactive power are both maintained by this FACTS device.

3.5. Wind Power Integration for the Improvement of VSM

The incorporation of wind power into the system can slightly increase the system's loadability. When the bus, which is most susceptible to voltage instability or a potential voltage collapse point, is integrated with the wind system, the voltage level stabilizes itself. The wind energy system is accessible in the PSAT Simulink library along with various induction generator (IG) configurations integrated with the IEEE-14 bus system. In the IEEE 14-bus test system used in this work, only generators 1 (slack bus) and 2 can generate both active and reactive power. Also, only reactive power is added to the system by the synchronous compensators connected with buses 3, 6, and 8. Instead of replacing the synchronous generators and compensators, in this paper, the Doubly-Fed Induction Generator-based Wind Energy Conversion System (DFIG-WECS) is connected to the system via the most critical bus.

3.6. Algorithm to Improve Loadability with STATCOM, SSSC, and UPFC

1. Run continuation power flow (CPF) for different values of k and each line outage. Perform raking based on the value of $\lambda_{\max}$.
2. Select some top cases having the lowest system loading parameter for *k* = 0.2, 0.5, 1.0, and 1.2 values.
3. Find out the BVSI and Cd value for all buses and all values of *k*. The most severe bus is the bus with the lowest BVSI and Cd values.
4. Calculate line stability indices (Lmn, FVSI, and Lqp) for all lines connected to the most critical bus obtain in step 3. The most severe line is that which has the highest value of line indices.
5. Place the FACTS devices at the most critical bus/line with wide variations in load pattern with/without wind power integration.
   a. Place the STATCOM at the most critical bus, obtain the system loading parameter by CPF and note down the value of the system loadability factor.
   b. Place the SSSC in the most critical line as selected in step 4, obtain the system loading parameter and note down the value of the system loadability factor.
   c. Place the shunt converter of the UPFC at the most severe bus as obtained in step 3 and the series convertor of the UPFC in the most critical line connected with the most severe bus, obtain the system loading parameter and note down the value of the system loadability factor.
6. Calculate the active and reactive power loadability of the critical load bus using (1) and (2) at the nose point with and without placement of the FACTS device and compare.
7. Plot the nose curve with and without using FACTS devices for the case which has maximum improvement in loadability.

Table 1. Line data of IEEE-14 bus test system

Line No.	Bus Number		Resistance (r) (in p.u.)	Reactance (x) (in p.u.)	Impedance Angle (θ) (in deg.)
	From	To			
1	6	12	0.12291	0.25581	64.33693
2	2	5	0.05695	0.17388	71.86509
3	7	9	0	0.11001	90
4	3	4	0.06701	0.17103	68.60463
5	11	10	0.08205	0.19207	66.86841
6	9	14	0.12711	0.27038	64.82103
7	3	2	0.04699	0.19797	76.64742
8	6	13	0.06615	0.13027	63.07893
9	5	4	0.01335	0.04211	72.40999
10	1	2	0.01938	0.05917	71.86478
11	4	7	0	0.20912	90
12	5	1	0.05403	0.22304	76.38278
13	5	6	0	0.25202	90
14	9	10	0.03181	0.0845	69.37117
15	2	4	0.05811	0.17632	71.75927
16	14	13	0.17093	0.34802	63.84204
17	12	13	0.22092	0.19988	42.13759
18	6	11	0.09498	0.1989	64.47429
19	8	7	0	0.17615	90
20	4	9	0	0.55618	90

4. RESULTS AND DISCUSSIONS

The effect of the STATCOM, SSSC, and UPFC on VSM and maximum real and reactive power loadability of the critical load bus have been investigated on IEEE-14 bus and functional Northern Region Power Grid (NRPG)-246 bus system. For both the test systems, the maximum loading parameter, $\lambda_{\max}$ has been evaluated for different values of k using CPF. Based on the maximum loadability of the test system, the line outage contingencies have been ranked. In this work, four values of k (0.2, 0.5, 1.0, and 1.2) have been considered for investigating the proposed method. Critical contingencies have been evaluated with wide variations in load patterns. The most critical bus has been found based on calculated BVSI and C_d indices values, and the validation of the method developed is done by comparing the critical buses as found in [40]. The most critical line has been found based on calculated Lmn, FVSI, and Lqp values. The validation of the method developed is done by comparing critical lines as found in [41]. The shunt FACTS device STATCOM is connected at the most severe bus and series FACTS devices SSSC, as well as the series component of the UPFC, are connected in the most critical line. Maximum loadability of the critical load bus has been obtained in different operating scenarios. The voltage vs loadability curve is plotted with and without FACTS devices.

4.1. IEEE-14 Bus System

This system consists of 14 buses, 20 lines having three transformers, a zero-injection bus at bus 7, 3 synchronous condensers at buses 3, 6, and 8, and 2 generators at buses 1 and 2 as shown in Fig. 3 [42]. The line connected between buses, The lines 2-5, 6-12, 12-13, 6-13, 6-11, 11-10, 9-10, 9-14, 14-13, 7-9, 1-2, 5-1, 3-2, 3-4, 5-4, 2-4, 4-9, 5-6, 4-7, and 8-7 (from the bus-to bus) are indexed as lines as shown in Table 1.

For all the lines of the IEEE 14-bus test system intact, the critical bus may be identified based on the value of BVSI and Cd for different values of k and listed in Table 2. It is observed that bus number 14 has the lowest indices value for all four types of load patterns. As a result, bus 14 is regarded as the IEEE-14 bus system's weakest bus. Also, in [33], [35], [40], and [43], bus number 14 was found as the most severe bus of the system from different methods. For this critical bus 14, the line connected between bus 14 and 13 is identified as the critical line on the basis of three indices, namely, Lmn, FVSI, and Lqp for different values of k. In a similar manner, critical buses and lines may be identified for line outage contingencies.

Table 2. Most severe bus and their bus voltage stability indices with different system loading

Loading Multiplier 'k'	Most Severe Bus	BVSI Value	Cd Value	$\lambda_{\max}$ of the System
0.2	14	0.11071	0.43669	4.21
0.5	14	0.11064	0.43668	4.16
1.0	14	0.11031	0.43644	4.03
1.2	14	0.10653	0.42815	3.96

Table 3. Ranking of top 5 critical line outage contingencies

R	k = 0.2		k = 0.5		k = 1.0		k = 1.2	
	LO	VSM	LO	VSM	LO	VSM	LO	VSM
1	1–2	1.343	1–2	1.341	1–2	1.336	1–2	1.334
2	3–2	2.289	3–2	2.279	3–2	2.261	3–2	2.215
3	5–6	2.557	5–6	2.454	5–6	2.279	5–6	2.253
4	2–4	3.37	7–9	3.341	7–9	2.883	7–9	2.689
5	2–5	3.539	2–4	3.343	6–13	3.220	6–13	3.052

LO = Line Outage, R = Ranking

Using CPF, the maximum loadability parameter λ has been obtained for all line outage cases at k = 0.2, 0.5, 1.0, and 1.2. Based on the value of $\lambda_{\max}$, all line outage contingency ranking has been performed for all values of k. The top three critical contingencies are independent of load pattern, k and are the same as evident from Table 3. However, the top five contingencies have been considered in this paper for further investigation.

For the top five-line outage contingencies, the critical bus has to be identified on the basis of BVSI and Cd for four different values of k. In Table 4, the most severe bus has been listed for the top five-line outage contingencies with k=0.2 and k=1.2. In all considered critical contingencies cases, the BVSI and Cd values of bus number 14 are found as lowest among all buses except in the case of line outage (3-2) at k=0.2. So, it is concluded that bus number 14 is found as the most severe bus also under considered contingencies. Therefore, bus 14 is the most suitable bus for the placement of shunt FACTS devices like STATCOM and the shunt part of the UPFC.

Critical bus 14 is connected to buses 9 and 13 only. Hence, for the critical line selection, only two lines (14-9 and 14-13) have been considered. For these two lines, three indices (Lmn, FVSI, and Lqp) have been evaluated for different values of k and are listed in Table 5. In most of the cases, line (14-13) has the highest line indices value except for line (6-13) outage cases. Hence, line (14-13) is considered to be the most critical line associated with the most critical bus 14 which was also found in [35] and [43] as the most severe line with different methodologies. This is the most optimal location for the placement of series FACTS devices like SSSC and series part of the UPFC.

As evident from Table IV, line (5-6) is one of the critical line outage contingencies. For this line outage, bus 14 is the critical bus, and line (14-13) is the critical line defined by the stability indices. For the critical line outage for line (5-6), the stability indices for the rest of the line have been represented pictorially for the IEEE-14 bus system at different values of k. It is also observed

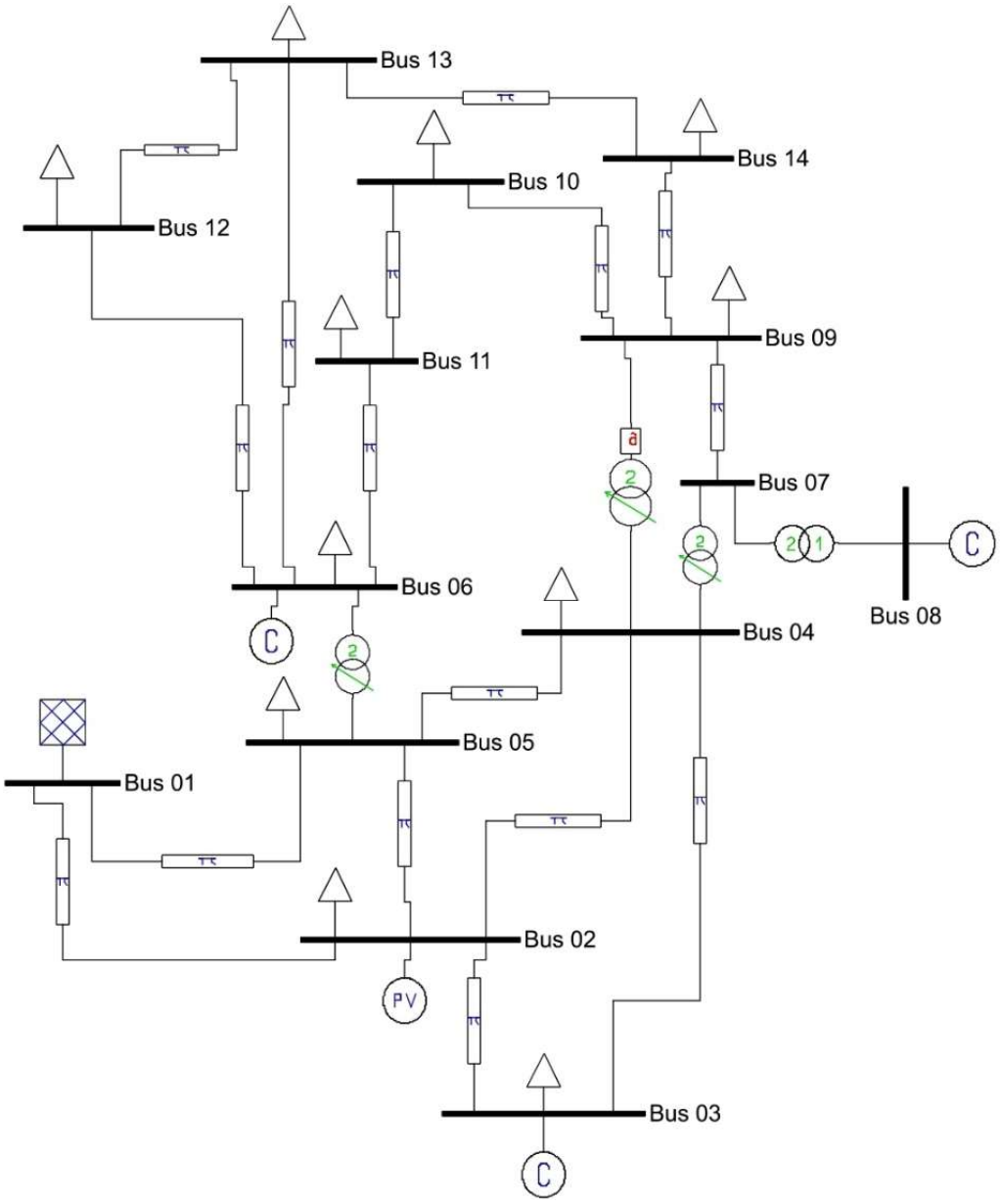

Fig. 3. IEEE-14 test bus system

Table 4. Most severe buses and their bus voltage stability indices under different contingencies

k=0.2				*k*=1.2			
Line Outage	**Most Severe Bus**	**BVSI Value**	**Cd Value**	**Line Outage**	**Most Severe Bus**	**BVSI Value**	**Cd Value**
1–2	14	0.10651	0.43051	1–2	14	0.09163	0.41508
3–2	3	0.10214	0.42184	3–2	14	0.09084	0.41068
5–6	14	0.11031	0.42961	5–6	14	0.09849	0.41934
2–4	14	0.11016	0.42778	7–9	14	0.09751	0.41733
2–5	14	0.10946	0.42703	6–13	14	0.09446	0.41644

that line (14-13) has the highest stability index value in the case of line outage (5-6) for different values of k.

After placing the STATCOM at the most severe bus number 14, the line indices values of the sever line (14-13) associated with this bus, get reduced as shown in Table 6. As a result, the severity of the critical line decreased. Also, in the cases of placement of SSSC and UPFC at the optimal locations, the line indices value for the severe line (14-13) has been decreased. Consequently, the severity of the line (14-13) gets also reduced.

The critical bus/line for the critical line outage has been identified for the placement of FACTS devices for the enhancement of voltage stability. In this paper, three FACTS devices, namely, SSSSC, STATCOM, and UPFC have been considered for this purpose. For the most critical line outage (between buses 5 and 6), STATCOM and shunt part of UPFC is located at severe bus i.e., bus 14 and SSSC, and the series part of the UPFC is placed at the most severe line (14-13) connected to most severe bus 14 of the IEEE-14 bus system. In the cases of wind integration and with the deployment of STATCOM at bus 14, the severity of the most severe bus 14 is no more severe and in this case, bus 5 is identified as the most severe bus as evident from Table 7. Also, the most severe bus of the system changed from bus number 14 to bus number 5 after the placement of UPFC at bus 14 as shown in Table 8. In general, SSSC should be placed at the most critical line but, in this paper, the SSSC has been placed in the severe line associated with the most critical bus 14. Therefore, the severity of the line (14-13) associated with the most critical bus 14 may not be affected upon placement of SSSC in the line (14-13).

The FACTS devices like STATCOM or shunt part of UPFC is placed at bus 14 and SSSC or series part of UPFC is placed at line 14-13. Also in similar manner, wind power is integrated with the most severe bus 14. For the top 5 lines outage cases (listed in Table 4 having the lowest voltage stability margin, the maximum loadability limit, $\lambda_{\max}$ has been evaluated with and without FACTS device at different values of k (k=0.2, 0.5, 1.0, and 1.2) as shown in Table 9, Table 10, Table 11, and Table 12.

From these Tables (from Table 9 to 12), the improvement in the VSM has been visible with the deployment of wind power and FACTS devices for different values of k. For the base case, the value of maximum loadability with FACTS devices deployed is also improved for different values of k, which is also reflected in [43]. In the intact case of using STACOM at bus number 14, the maximum loadability has been increased from 4.03 p.u. to 4.10 p.u. as shown in Table 11. Whereas in the same case, it was increased up to only 4.08923 p.u. in [43]. In the same scenario when UPFC is used the maximum loadability gets improved from 4.03 p.u. to 4.17 whereas it was improved only up to 4.10391 p.u. in [43] as shown in Table 13. From these tables, it is observed that in all these line outage cases with the intact case at different values of k (k=0.2, 0.5, 1.0, 1.2), the system loadability factor has been increased when the FACTS devices are used in the system. Also, the maximum real and reactive power demand at the most critical bus 14 gets improved. It is found that in the line outage case (7-9) at multiplier value k=1.0, the gap between the system loadability factor with and without FACTS devices is maximum in comparison to other cases. Thereby in this case the gap between maximum real and reactive power demand with and without FACTS devices is maximum in comparison to other cases. The maximum loading factor $\lambda_{\max}$ (in p.u.) with and without FACTS devices at k=1.0 (base case) has been comprised with other research is shown in Table 13.

The value of the system loadability factor with line outage (7-9) and without FACTS device at multiplier value k=1.0 is 2.88, whereas its value gets improved by 3.48 p.u., 2.95 p.u., 3.51 p.u., and 3.55p.u. when SSSC, STATCOM, combined SSSC and STATCOM, and UPFC are placed at the most critical line and bus respectively. Similarly, the maximum real and reactive power demand with line outage (7-9) and without FACTS device at multiplier value k=1.0 is 57.86 MW and 19.42 MVAR, whereas its

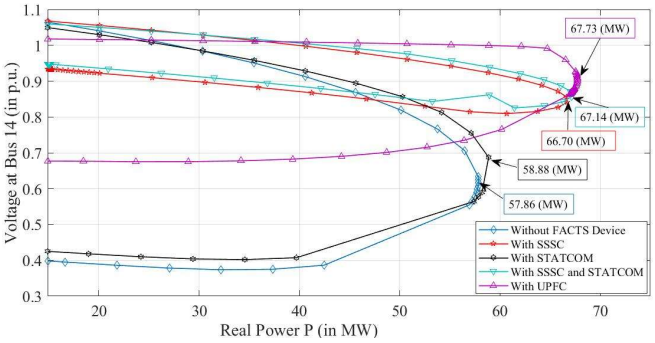

Fig. 4. Real power demand vs voltage at bus 14 with k=1 for line outage 7–9

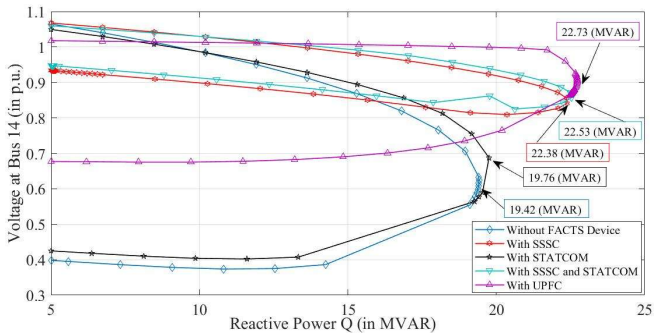

Fig. 5. Reactive power demand vs voltage at bus 14 with k=1 for line outage 7–9

value gets improved by 66.70 MW and 22.38 MVAR, 58.88 MW and 19.76 MVAR, 67.14 MW and 22.53 MVAR as well as 67.73 MW and 22.73 MVAR when SSSC, STATCOM combined SSSC and STATCOM, as well as UPFC, are placed at the most critical line and bus respectively as shown in Fig. 4 and Fig. 5.

4.2. NRPG-246 Bus System

India has five regional electricity grids, with the Northern Region Power Grid (NRPG)-246 being the largest [44]. This system consists of 376 lines including transformer branches, and 246 buses at 220 kV and 400 kV. The critical buses for intact cases with variations in load pattern, k are identified based on BVSI, and Cd values as shown in Table 14. It is observed that under lightly loading conditions (k=0.2), bus number 242 is identified as the critical bus of the NRPG-246 system, whereas bus number 173 is found as the most stressed bus for other loading patterns (k=0.5, 1.0, and 1.2).

The maximum loadability parameter $\lambda_{\max}$ has been calculated using continuation power flow for all line outage scenarios at k = 0.2, 0.5, 1.0, and 1.2. Contingency ranking has been done based on VSM for all chosen values of k as shown in Table 15. From Table 15, it is seen that line outages 61-154, 156-158, 40-41, 166-173, 173-174, 165-174, 219-77, 181-158, 160-164, 106-123, 168-171, 158-160, and 165-171 are the critical contingency with wide variation in load pattern. The VSM obtain in Table 15 in different contingencies and different load patterns are compared with the results obtained in [45] as shown in Table 16.

The BVSI and Cd values for all buses have been calculated considering critical contingencies and wide variation in load patterns using load flow analysis data. For the top ten-line outage contingencies, a critical bus must be identified on the basis of BVSI and Cd for four different values of k. In Table 17, the most severe bus has been listed for the top ten-line outage contingencies with k=0.5 and k=1.2. In most of the considered critical contingencies

Table 5. Line voltage stability indices at different contingencies with wide variation in load pattern '*k*'

Line Outage		*k*=0.2			*k*=0.5			*k*=1.0			*k*=1.2		
	Line	Lmn	FVSI	Lqp	Lmn	FVSI	Lqp	Lmn	FVSI	Lqp	Lmn	FVSI	Lqp
Intact Case	14–13	0.0679	0.0692	0.0529	0.03	0.0306	0.0223	0.0637	0.0649	0.055	0.0839	0.0854	0.0659
	14–9	0.0138	0.0136	0.0124	0.0098	0.0097	0.0093	0.0154	0.0152	0.0112	0.0154	0.0152	0.0137
2–1	14–13	0.0122	0.0125	0.0063	0.0339	0.0349	0.024	0.0725	0.0744	0.0553	0.0889	0.0911	0.0685
	14–9	0.0063	0.0062	0.0058	0.0085	0.0084	0.0076	0.0124	0.0122	0.0107	0.0139	0.0138	0.0119
3–2	14–13	0.0089	0.0091	0.0045	0.0304	0.0311	0.0219	0.0686	0.0701	0.0528	0.0847	0.0865	0.0659
	14–9	0.008	0.0078	0.0075	0.0103	0.0101	0.0093	0.0142	0.014	0.0124	0.0158	0.0156	0.0137
5–6	14–13	**0.14**	**0.133**	**0.102**	**0.168**	**0.159**	**0.123**	**0.217**	**0.205**	**0.159**	**0.239**	**0.224**	**0.175**
	14–9	0.1369	0.1348	0.0581	0.1251	0.1230	0.046	0.1496	0.1566	0.1323	0.1631	0.1710	0.1441
2–4	14–13	0.0136	0.0139	0.0083	0.0355	0.0363	0.0261	—	—	—	—	—	—
	14–9	0.0043	0.0043	0.0046	0.0064	0.0063	0.0062	—	—	—	—	—	—
2–5	14–13	0.0172	0.0175	0.0122	—	—	—	—	—	—	—	—	—
	14–9	0.0006	0.0006	0.0021	—	—	—	—	—	—	—	—	—
7–9	14–13	—	—	—	0.061	0.0636	0.0411	0.134	0.1391	0.1002	0.1661	0.1723	0.1261
	14–9	—	—	—	0.0063	0.0063	0.0051	0.0253	0.0253	0.0207	0.0337	0.0337	0.0276
6–13	14–13	—	—	—	—	—	—	0.019	0.019	0.016	0.017	0.017	0.014
	14–9	—	—	—	—	—	—	0.079	0.077	0.069	0.091	0.089	0.078

Table 6. Line Stability Indices of Line (14-13) with and without placing the STATCOM, SSSC, and UPFC for the line outage (5-6)

Loading Multiplier '*k*'	Without FACTS			With STATCOM at Bus 14			With SSSC in Line (14-13)			With UPFC at Among Bus 14 and Line (14-13)		
	Lmn	FVSI	Lqp	Lmn	FVSI	Lqp	Lmn	FVSI	Lqp	Lmn	FVSI	Lqp
0.2	0.14	0.133	0.102	0.117	0.118	0.094	0.096	0.098	0.073	0.075	0.071	0.069
0.5	0.168	0.159	0.123	0.151	0.142	0.114	0.118	0.135	0.082	0.098	0.096	0.081
1.0	0.217	0.205	0.159	0.196	0.183	0.138	0.131	0.142	0.103	0.105	0.113	0.091
1.2	0.239	0.224	0.175	0.209	0.202	0.149	0.143	0.139	0.109	0.112	0.099	0.105

Table 7. The most severe bus with STATCOM/wind integration deployed at bus 14

Loading Multiplier '*k*'	Without FACTS/Wind Integration			With Wind Integration at 14^{th} Bus			With STATCOM at 14^{th} Bus		
	Most Severe Bus	BVSI Value	Cd Value	Most Severe Bus	BVSI Value	Cd Value	Most Severe Bus	BVSI Value	Cd Value
0.2	14	0.11071	0.43669	5	0.12248	0.46052	5	0.12817	0.46384
0.5	14	0.11064	0.43668	5	0.12201	0.45951	5	0.12691	0.46076
1.0	14	0.11031	0.43644	5	0.12139	0.45821	5	0.12534	0.45944
1.2	14	0.10653	0.42815	5	0.12108	0.45741	5	0.12183	0.45879

Table 8. The most severe bus with UPFC deployed at bus 14 and line (14-13)

Loading Multiplier '*k*'	Without UPFC			With UPFC		
	Most Severe Bus	BVSI Value	Cd Value	Most Severe Bus	BVSI Value	Cd Value
0.2	14	0.11071	0.43669	5	0.12765	0.46147
0.5	14	0.11064	0.43668	5	0.12596	0.45957
1.0	14	0.11031	0.43644	5	0.12507	0.45885
1.2	14	0.10653	0.42815	5	0.12029	0.45796

Table 9. Maximum loading factor λ_{max} (in p.u.) with and without FACTS devices at k=0.2

Line Outage	λ_{max} without FACTS	λ_{max} with wind integration	λ_{max} with SSSC	λ_{max} with STATCOM	λ_{max} with SSSC and STATCOM	λ_{max} with UPFC
Intact Case	4.21	4.215	4.25	4.23	4.26	4.27
1–2	1.34	1.345	1.35	1.34	1.35	1.35
3–2	2.29	2.301	2.30	2.29	2.31	2.31
5–6	2.56	2.564	2.75	2.61	2.78	2.86
2–4	3.37	1.374	3.39	3.38	3.40	3.40
2–5	3.54	3.545	3.56	3.55	3.57	3.58
7–9	**3.59**	**3.5936**	**3.87**	**3.65**	**3.88**	**3.93**
6–13	3.88	3.8847	3.89	3.95	3.95	4.09

Table 10. Maximum loading factor λ_{max} (in p.u.) with and without FACTS devices at k=0.5

Line Outage	λ_{max} without FACTS	λ_{max} with wind integration	λ_{max} with SSSC	λ_{max} with STATCOM	λ_{max} with SSSC and STATCOM	λ_{max} with UPFC
Intact Case	4.16	4.1618	4.21	4.18	4.18	4.24
1–2	1.34	1.3424	1.34	1.34	1.34	1.34
3–2	2.28	2.2784	2.30	2.28	2.28	2.30
5–6	2.45	2.4531	2.66	2.51	2.51	2.77
2–4	3.34	3.3403	3.37	3.35	3.35	3.39
2–5	3.50	2.5072	3.53	3.52	3.52	3.55
7–9	**3.34**	**3.346**	**3.76**	**3.42**	**3.42**	**3.83**
6–13	3.64	3.6555	3.65	3.75	3.75	4.03

Table 11. Maximum loading factor λ_{max} (in p.u.) with and without FACTS devices at k=1.0

Line Outage	λ_{max} without FACTS	λ_{max} with wind integration	λ_{max} with SSSC	λ_{max} with STATCOM	λ_{max} with SSSC and STATCOM	λ_{max} with UPFC
Intact Case	4.03	4.0356	4.12	4.10	4.13	4.17
1–2	1.34	1.3446	1.34	1.34	1.34	1.34
3–2	2.26	2.2655	2.28	2.27	2.28	2.29
5–6	2.28	2.286	2.50	2.34	2.52	2.62
2–4	3.28	3.291	3.32	3.30	3.33	3.35
2–5	3.42	3.431	3.47	3.45	3.48	3.50
7–9	**2.88**	**2.8967**	**3.48**	**2.95**	**3.51**	**3.55**
6–13	3.22	3.226	3.23	3.33	3.66	3.79

Table 12. Maximum loading factor λ_{max} (in p.u.) with and without FACTS devices at k=1.2

Line Outage	λ_{max} without FACTS	λ_{max} with wind integration	λ_{max} with SSSC	λ_{max} with STATCOM	λ_{max} with SSSC and STATCOM	λ_{max} with UPFC
Intact Case	3.96	3.968	4.08	4.00	4.09	4.13
1–2	1.33	1.3401	1.34	1.34	1.34	1.34
3–2	2.25	2.256	2.28	2.26	2.28	2.28
5–6	2.22	2.227	2.43	2.28	2.46	2.56
2–4	3.25	3.254	3.30	3.27	3.31	3.33
2–5	3.38	3.388	3.44	3.41	3.45	3.47
7–9	2.69	2.702	3.33	2.76	3.36	3.33
6–13	3.05	3.057	3.06	3.16	3.59	3.64

Table 13. Comparison of maximum loading factor λ_{max} (in p.u.) with and without FACTS devices at k=1.0 (base case)

λ_{max} without FACTS	λ_{max} with STATCOM (Proposed Approach)	λ_{max} with STATCOM (Found in [43])	λ_{max} with UPFC (Proposed Approach)	λ_{max} with UPFC (Found in [43]
4.03	4.10	4.08923	4.17	4.10391

Table 14. Most severe buses and their bus voltage stability indices with different system loading

Loading Multiplier '*k*'	Most Severe Bus	BVSI Value	Cd Value
0.2	242	0.06249	0.17164
0.5	173	0.07416	0.19467
1.0	173	0.07298	0.19386
1.2	173	0.06778	0.19377

Table 15. Ranking of top 10 critical contingencies

R	*k* = 0.2		*k* = 0.5		*k* = 1.0		*k* = 1.2	
	LO	VSM	LO	VSM	LO	VSM	LO	VSM
1	61–154	0.092	156–158	0.07	156–158	0.343	156–158	0.394
2	156–158	0.197	40–41	0.929	173–174	1.058	173–174	0.991
3	40–41	0.750	173–174	1.252	40–41	1.081	165–174	1.091
4	166–173	1.102	165–174	1.392	165–174	1.167	40–41	1.097
5	173–174	1.394	181–158	1.503	181–158	1.296	181–158	1.225
6	165–174	1.554	219–77	1.507	160–164	1.311	160–164	1.235
7	219–77	1.631	160–164	1.529	168–171	1.37	168–171	1.291
8	181–158	1.642	168–171	1.59	219–77	1.374	219–77	1.352
9	160–164	1.6860	106–123	1.613	158–160	1.446	158–160	1.365
10	106–123	1.7313	158–160	1.675	165–171	1.471	165–171	1.381

cases, the BVSI and Cd values of bus number 173 are found as lowest among all buses at k=0.5 and 1.2. Hence, bus number 173 is considered to be the weakest bus which is the same bus associated with the most critical line found in [41]. This bus 173 is the most appropriate bus for the placement of shunt FACTS devices like STATCOM and the shunt component of the UPFC.

Similarly, the line indices Lmn, FVSI, and Lqp values are calculated for the lines (166-173) and (173-174) which are associated with the weakest bus number 173 for different values of k as depicted in Table 18. Among all cases, line (166-173) has the highest line indices value. So, it is concluded that the most critical line (166-173), is connected to the most severe bus which same as found in [41]. And this is the most optimal location for the placement of series FACTS devices like SSSC and series part of the UPFC.

The wind power integration and the FACTS devices, namely, SSSSC, STATCOM, and UPFC have been placed at the most severe line (166-173), most critical bus number 173, and among the most severe line and bus of the system respectively for the NRPG-246 bus system.

In the cases of the deployment of the wind power and STATCOM at bus 173, the severity of the most severe bus 173 is no more severe and in this case, bus 242 is observed as the most severe bus in the system as shown in Table 19. Also, the severity of bus 173 become dismissed after placing the UPFC at bus 173, and the most severe bus of the system changed from bus number 173 to bus number 242 as shown in Table 19. In general, SSSC should be placed at the most critical line but, in this paper, the SSSC has been placed in the severe line associated with the most critical bus 173. Therefore, the severity of the line (166-173) associated with the most critical bus 173 may not be affected upon placement of SSSC in the line (166-173).

For the top 10 severe lines outage cases along with the intact case having the lowest voltage stability margin, the maximum demand limit at bus number 173 has been evaluated with and without FACTS device: the SSSC, the STATCOM, combined SSSC, and STATCOM, and the UPFC at different values of k (k=0.2, 0.5, 1.0, 1.2). Table 20 and Table 21 show the Maximum loading limit ($\lambda_{\max}$) with and without using FACTS devices at k=0.5 and 1.2, respectively. With the integration of wind power at bus 173 (critical bus), there is no significant effect on maximum

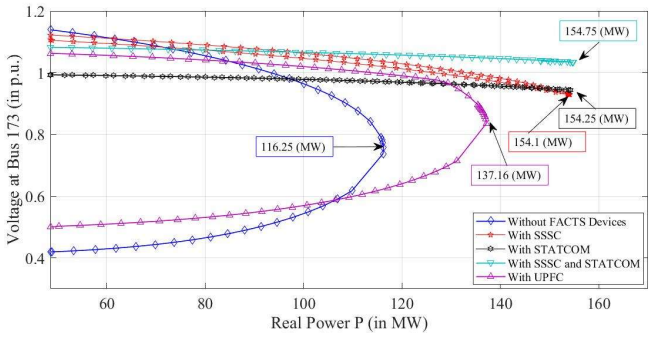

Fig. 6. Real power demand vs voltage curve at 173rd bus at k=0.5 for line outage 165-174

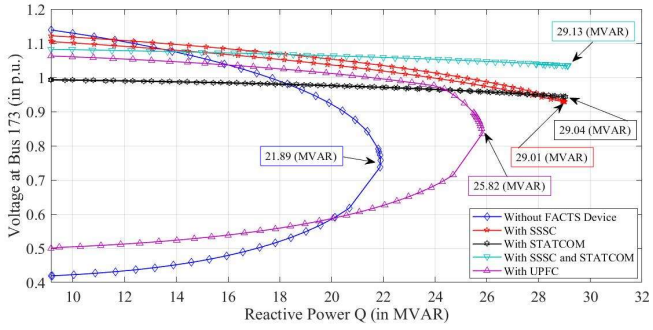

Fig. 7. Reactive power demand vs voltage curve at 173rd bus at k=0.5 for line outage 165-174

loadability ($\lambda_{\max}$), but its effect is seen on voltage stability indices BVSI and Cd as shown in Table 19. As a result, after the deployment of wind power at bus 173, the most critical bus has been changed from bus 173 to bus 242.

From Tables 20 and 21, it is observed that in all these line outage cases with the intact case at different values of k=0.2, 0.5, 1.0, and 1.2, the system loadability factor ($\lambda_{\max}$) has been increased on the deployment of FACTS devices. Hence, the maximum real and reactive power demand limit at the most critical bus 173 gets improved. It is found that in the line outage case (165-174) at multiplier value k=0.5, the gap between the system loadability factor with and without FACTS devices is maximum in comparison to other cases. Thereby in this case the gap between maximum real and reactive power demand with and without FACTS devices is maximum in comparison to other cases.

The value of the system loadability factor with line outage (165-174) and without FACTS device at multiplier value k=0.5 is 1.39 p.u., whereas its value gets improved by 2.17 p.u., 2.17 p.u., and 1.82 p.u. when SSSC, STATCOM, and UPFC are placed at the most critical line and bus respectively. Similarly, the maximum real and reactive power demand with line outage (165-174) and without FACTS device at multiplier value k=0.5 are 116.25 MW and 21.89 MVAR, whereas its value gets improved by 154.1 MW and 29.01 MVAR, 154.25 MW and 29.04 MVAR, 154.75 MW and 29.13 MVAR, as well as 137.16 MW and 25.82 MVAR when SSSC, STATCOM combined SSSC and STATCOM, as well as UPFC, are placed at the most critical line and bus, respectively as shown in Fig. 6 and Fig. 7.

Table 16. Comparison of voltage stability margin under top 10 critical contingencies with wide variations in load Patterns

k = 0.2			k = 0.5			k = 1.0			k = 1.2		
LO	**VSM**	**VSM [45]**	**LO**	**VSM**	**VSM [45]**	**LO**	**VSM**	**VSM [45]**	**LO**	**VSM**	**VSM [45]**
61–154	0.092	NE	156–158	0.07	NE	156–158	0.343	0.34	156–158	0.394	0.39
156–158	0.197	0.19	40–41	0.929	0.92	173–174	1.058	1.05	173–174	0.991	0.99
40–41	0.750	0.75	173–174	1.252	1.25	40–41	1.081	1.08	165–174	1.091	1.09
166–173	1.102	1.10	165–174	1.392	1.39	165–174	1.167	1.16	40–41	1.097	1.10
173–174	1.394	1.39	181–158	1.503	1.50	181–158	1.296	1.29	181–158	1.225	1.22
165–174	1.554	1.55	219–77	1.507	1.51	160–164	1.311	1.31	160–164	1.235	1.23
219–77	1.631	1.63	160–164	1.529	1.53	168–171	1.37	1.36	168–171	1.291	1.29
181–158	1.642	1.64	168–171	1.59	1.59	219–77	1.374	1.37	219–77	1.352	1.35
160–164	1.6860	1.68	106–123	1.613	1.61	158–160	1.446	NE	158–160	1.365	1.36
106–123	1.7313	1.73	158–160	1.675	1.67	165–171	1.471	1.47	165–171	1.381	1.38

NE = Not Evaluated

Table 17. Most severe buses and their bus voltage stability indices under different contingencies

k=0.5				k=1.2			
Line Outage	**Most Severe Bus**	**BVSI Value**	**Cd Value**	**Line Outage**	**Most Severe Bus**	**BVSI Value**	**Cd Value**
156–158	173	0.07015	0.18521	156–158	173	0.06224	0.18288
40–41	173	0.07083	0.18846	173–174	173	0.06281	0.18691
173–174	173	0.07124	0.18851	165–174	174	0.06334	0.18712
165–174	174	0.07211	0.18903	40–41	173	0.06346	0.18756
181–158	173	0.07243	0.19062	181–158	173	0.06609	0.19034
219–77	173	0.07271	0.19297	160–164	173	0.06723	0.19161
160–164	173	0.07272	0.19467	168–171	173	0.06951	0.19543
168–171	173	0.07281	0.19573	219–77	173	0.07084	0.19261
106–123	173	0.07302	0.19362	158–160	173	0.07132	0.19315
158–160	173	0.07305	0.19352	165–171	173	0.07186	0.19289

Table 18. Line voltage stability indices at different contingencies with wide variation in load pattern k

Line Outage	**Line Number**	k=0.2			k=0.5			k=1.0			k=1.2		
		Lmn	**FVSI**	**Lqp**	**Lmn**	**FVSI**	**Lqp**	**Lmn**	**FVSI**	**Lqp**	**Lmn**	**FVSI**	**Lqp**
Intact Case	166–173	0.597	0.601	0.769	0.594	0.598	0.768	0.606	0.610	0.420	0.587	0.591	0.763
	173–174	0.484	0.480	0.475	0.493	0.488	0.483	0.581	0.576	0.540	0.513	0.507	0.503
40–41	166–173	0.572	0.575	0.797	0.569	0.569	0.796	0.564	0.567	0.793	0.561	0.565	0.791
	173–174	0.484	0.480	0.475	0.492	0.492	0.483	0.506	0.501	0.496	0.512	0.507	0.503
156–158	**166–173**	**0.598**	**0.602**	**0.769**	**0.595**	**0.689**	**0.869**	**0.590**	**0.595**	**0.765**	**0.588**	**0.593**	**0.763**
	173–174	0.488	0.484	0.478	0.497	0.493	0.487	0.511	0.507	0.501	0.518	0.513	0.508
165–174	166–173	0.597	0.601	0.769	0.594	0.599	0.768	0.589	0.593	0.764	0.587	0.591	0.763
	173–174	0.506	0.500	0.500	0.523	0.517	0.517	0.559	0.552	0.550	0.580	0.573	0.574
168–171	166–173	0.597	0.601	0.769	0.594	0.598	0.767	0.589	0.593	0.764	0.587	0.591	0.763
	173–174	0.492	0.484	0.497	0.496	0.492	0.487	0.510	0.506	0.501	0.517	0.512	0.508
173–174	166–173	0.597	0.601	0.769	0.594	0.598	0.767	0.589	0.593	0.764	0.587	0.591	0.763
	173–174	L.O.	L.O.	L.O.	L.O.	L.O.	L.O.	L.O.	L.O.	L.O.	L.O.	L.O.	L.O.
181–158	166–173	0.597	0.601	0.769	0.594	0.661	0.869	0.589	0.593	0.764	0.587	0.591	0.763
	173–174	0.486	0.482	0.476	0.523	0.578	0.573	0.507	0.502	0.497	0.513	0.508	0.503
219–77	166–173	0.597	0.601	0.770	0.594	0.598	0.768	0.589	0.593	0.764	0.587	0.591	0.763
	173–174	0.484	0.480	0.475	0.493	0.488	0.483	0.506	0.501	0.496	0.512	0.507	0.503
160–164	166–173	—	—	—	0.594	0.598	0.767	0.589	0.593	0.764	0.587	0.591	0.763
	173–174	—	—	—	0.512	0.504	0.517	0.549	0.540	0.555	0.567	0.558	0.573
158–160	166-173	—	—	—	0.594	0.598	0.767	0.589	0.593	0.764	0.561	0.660	0.875
	173–174	—	—	—	0.492	0.488	0.483	0.505	0.501	0.496	0.512	0.586	0.584

Table 19. The most severe bus with STATCOM/wind integration deployed at bus 173 and UPFC deployed at bus 173 and line (166-173).

Loading Multiplier '*k*'	Without FACTS			With Wind Integration at 173^{rh} Bus			With STATCOM at 173^{rh} Bus			With UPFC (at Bus 173 and Line 166-173)		
	Most Severe Bus	BVSI Value	Cd Value	Most Severe Bus	BVSI Value	Cd Value	Most Severe Bus	BVSI Value	Cd Value	Most Severe Bus	BVSI Value	Cd Value
0.2	242	0.06249	0.17164	242	0.06295	0.17324	242	0.06318	0.17551	242	0.06304	0.17536
0.5	173	0.07416	0.19467	242	0.06269	0.17298	242	0.06297	0.17372	242	0.6281	0.17402
1.0	173	0.07298	0.19386	242	0.06255	0.17185	242	0.06275	0.17281	242	0.06268	0.17212
1.2	173	0.06778	0.19377	242	0.06249	0.17111	242	0.06252	0.17173	242	0.06265	0.17131

Table 20. Maximum loading limit ($\lambda_{\max}$) (in p.u.) with and without using FACTS devices at k =0.5

Line Outage	$\lambda_{\max}$ without FACTS	$\lambda_{\max}$ with SSSC	$\lambda_{\max}$ with STATCOM	$\lambda_{\max}$ with SSSC and STATCOM	$\lambda_{\max}$ with UPFC
Intact Case	2.17	2.18	2.18	2.18	2.18
40–41	0.93	0.97	0.94	0.97	0.97
156–158	0.07	0.10	0.08	0.10	0.13
158–160	1.67	1.68	1.68	1.68	1.68
160–164	1.53	1.54	1.61	1.73	1.58
165–174	**1.39**	**2.17**	**2.17**	**2.18**	**1.82**
168–171	1.59	1.61	1.61	1.62	1.61
173–174	1.25	1.26	1.26	1.26	1.26
181–158	1.50	1.51	1.52	1.54	1.52
219–77	1.51	1.55	1.52	1.55	1.53
106–123	1.61	1.65	1.62	1.65	1.64

Table 21. Maximum loading limit ($\lambda_{\max}$) (in p.u.) with and without using FACTS devices at k=1.2

Line Outage	$\lambda_{\max}$ without FACTS	$\lambda_{\max}$ with SSSC	$\lambda_{\max}$ with STATCOM	$\lambda_{\max}$ with SSSC and STATCOM	$\lambda_{\max}$ with UPFC
Intact Case	1.75	1.78	1.78	1.79	1.78
40–41	1.10	1.15	1.10	1.14	1.14
156–158	0.39	0.42	1.39	0.41	0.46
158–160	1.36	1.37	1.37	1.37	1.37
160–164	1.23	1.23	1.28	1.35	1.26
165–171	1.38	1.39	1.39	1.39	1.38
165–174	1.09	1.77	1.73	1.78	1.46
168–171	1.29	1.31	1.30	1.32	1.30
173–174	0.99	0.99	0.99	1.02	0.99
181–158	1.23	1.23	1.23	1.23	1.23
219–77	1.35	1.46	1.35	1.45	1.35

5. CONCLUSIONS

In this paper, the voltage stability margin of the most critical lines and buses of the IEEE-14 bus and NRPG-246 bus systems is examined in relation to the effects of series and shunt FACTS devices like SSSC, STATCOM, and UPFC. A simple and fast approach has been developed to achieve this. Four types of load patterns have been considered for both systems. Among these load patterns, five and ten types of line outage cases based on the lowest maximum loadability factor have been taken for further analysis for the IEEE-14 bus and NRPG-246 bus systems respectively. With the wide variation in load patterns and critical contingencies, critical boundary index and degree centrality measurement methods have been used to determine the most severe line of both systems. With the wide variation in load pattern and for critical contingencies, the line stability indices, Lqp, Lmn, and FVSI methods have been used to find the most severe line of both systems. When FACTS devise SSSC, STATCOM and UPFC are placed at the most severe lines and critical load buses, results show an increase in maximum loadability of the system and hence enhancement in voltage stability margin of the most severe buses 14 and 173 of IEEE-14 bus and NRPG-246 bus system respectively in all considered cases as expected. For the IEEE-14 bus system, the improvement in voltage stability margin for critical line outages at all load patterns is evident with deployment for FACTS devices placed at optimal location in the system as evident from Tables 9, 10, 11, and 12. Similar improvement in VSM is also reported for the NRPG-246 bus system (refer Tables 20 and 21). With the

deployment of the FACTS devices at optimal location, considerable improvement in VSM has been observed for critical contingencies at all load patterns.

REFERENCES

[1] H. Saadat, "Power systems analysis 2nd edition-psa," 2009.

[2] C.W. Taylor, "Voltage stability," *Power System Voltage Stability*, pp. 27–32, 1994.

[3] C.A. Canizares, "Voltage stability assessment: concepts, practices and tools," *IEEE/PES Power System Stability Subcommittee Special Publication*, no. SP101PSS, 2002.

[4] S. Sao, "Voltage stability indicator at the proximity of the voltage collapse point and its implication on margin," *Asian J. Comput. Sci. Inf. Technol.*, vol. 5, pp. 151–154, 2011.

[5] N. Hatziargyriou, J. van Hecke, T. van Cutsem, I.C. on Large High Voltage Electric Systems Study Committee Power System Analysis, T.W. G.T. Force, I.C. on Large High Voltage Electric Systems. WG 38/02. Task Force 11, and I.C. on Large High Voltage Electric Systems. Working Group 38.02. Task Force 11, *Indices Predicting Voltage Collapse Including Dynamic Phenomena*. Brochures thématiques: International Conference on Large High Voltage Electric Systems, CIGRE, 1994.

[6] P.S. Kundur and O.P. Malik, *Power System Stability and Control*. McGraw-Hill Education, 2022.

[7] G. Andersson, P. Donalek, R. Farmer, N. Hatziargyriou, I. Kamwa, P. Kundur, N. Martins, J. Paserba, P. Pourbeik, J. Sanchez-Gasca, *et al.*, "Causes of the 2003 major grid blackouts in north america and europe, and recommended means to improve system dynamic performance," *IEEE Trans. Power Syst.*, vol. 20, no. 4, pp. 1922–1928, 2005.

[8] V. Venikov, V. Stroev, V. Idelchick, and V. Tarasov, "Estimation of electrical power system steady-state stability in load flow calculations," *IEEE Trans. Power Appar. Syst.*, vol. 94, no. 3, pp. 1034–1041, 1975.

[9] P.-A. Lof, T. Smed, G. Andersson, and D. Hill, "Fast calculation of a voltage stability index," *IEEE Trans. Power Syst.*, vol. 7, no. 1, pp. 54–64, 1992.

[10] B. Gao, G. Morison, and P. Kundur, "Voltage stability evaluation using modal analysis," *IEEE Trans. Power Syst.*, vol. 7, no. 4, pp. 1529–1542, 1992.

[11] S. Konar, D. Chatterjee, and S. Patra, "V–q sensitivity-based index for assessment of dynamic voltage stability of power systems," *IET Gener. Transm. Distrib.*, vol. 9, no. 7, pp. 677–685, 2015.

[12] P. Kessel and H. Glavitsch, "Estimating the voltage stability of a power system," *IEEE Trans. Power Deliv.*, vol. 1, no. 3, pp. 346–354, 1986.

[13] I. Musirin and T.A. Rahman, "Novel fast voltage stability index (fvsi) for voltage stability analysis in power transmission system," in *Student conference on research and development*, pp. 265–268, IEEE, 2002.

[14] A. Mohamed, G. Jasmon, and S. Yusoff, "A static voltage collapse indicator using line stability factors," *J. Ind. Technol.*, vol. 7, no. 1, pp. 73–85, 1989.

[15] K. Vu, M.M. Begovic, D. Novosel, and M.M. Saha, "Use of local measurements to estimate voltage-stability margin," *IEEE Trans. Power Syst.*, vol. 14, no. 3, pp. 1029–1035, 1999.

[16] M. Sagara, R. Shigenobu, O.B. Adewuyi, A. Yona, T. Senjyu, M.S.S. Danish, and T. Funabashi, "Voltage stability improvement by demand response," in *TENCON 2017-2017 IEEE Region 10 Conference*, pp. 2144–2149, IEEE, 2017.

[17] S.M. Hur Rizvi, P. Kundu, and A.K. Srivastava, "Hybrid voltage stability and security assessment using synchrophasors with consideration of generator q-limits," *IET Gener. Transm. Distrib.*, vol. 14, no. 19, pp. 4042–4051, 2020.

[18] M. Mohammadniaei, F. Namdari, and M. Shahkarami, "A fast voltage collapse detection and prevention based on wide area monitoring and control," *J J. Oper. Autom. Power Eng.*, vol. 8, no. 3, pp. 209–219, 2020.

[19] P. Akbarzadeh Aghdam and H. Khoshkhoo, "Voltage stability assessment algorithm to predict power system loadability margin," *IET Gener. Transm. Distrib.*, vol. 14, no. 10, pp. 1816–1828, 2020.

[20] A. Alshareef, R. Shah, N. Mithulananthan, and S. Alzahrani, "A new global index for short term voltage stability assessment," *IEEE Access*, vol. 9, pp. 36114–36124, 2021.

[21] B. Ismail, N.I.A. Wahab, M.L. Othman, M.A.M. Radzi, K.N. Vijayakumar, M.K. Rahmat, and M.N.M. Naain, "New line voltage stability index (bvsi) for voltage stability assessment in power system: the comparative studies," *IEEE Access*, vol. 10, pp. 103906–103931, 2022.

[22] Z. Wang, A. Scaglione, and R.J. Thomas, "Electrical centrality measures for electric power grid vulnerability analysis," in *49th IEEE conference on decision and control (CDC)*, pp. 5792–5797, IEEE, 2010.

[23] E.P.R. Coelho, M.H.M. Paiva, M.E.V. Segatto, and G. Caporossi, "A new approach for contingency analysis based on centrality measures," *IEEE Syst. J.*, vol. 13, no. 2, pp. 1915–1923, 2018.

[24] F. Hussian, G.R. Goyal, A.K. Arya, and B.P. Soni, "Contingency ranking for voltage stability in power system," in *2021 IEEE International Conference on Electronics, Computing and Communication Technologies (CONECCT)*, pp. 1–4, IEEE, 2021.

[25] Y.G. Werkie and H.A. Kefale, "Optimal allocation of multiple distributed generation units in power distribution networks for voltage profile improvement and power losses minimization," *Cogent Eng.*, vol. 9, no. 1, p. 2091668, 2022.

[26] M. Kazeminejad, M. Banejad, U. Annakkage, and N. Hosseinzadeh, "The effect of high penetration level of distributed generation sources on voltage stability analysis in unbalanced distribution systems considering load model," *J. Oper. Autom. Power Eng.*, vol. 7, no. 2, pp. 196–205, 2019.

[27] S. Gerbex, R. Cherkaoui, and A.J. Germond, "Optimal location of multi-type facts devices in a power system by means of genetic algorithms," *IEEE Trans. Power Syst.*, vol. 16, no. 3, pp. 537–544, 2001.

[28] N.G. Hingorani and L. Gyugyi, *Understanding FACTS: concepts and technology of flexible AC transmission systems*. Wiley-IEEE Press, 2000.

[29] Y.-C. Chang, "Multi-objective optimal svc installation for power system loading margin improvement," *IEEE Trans. Power Syst.*, vol. 27, no. 2, pp. 984–992, 2011.

[30] C.-Y. Lee, S.-H. Tsai, and Y.-K. Wu, "A new approach to the assessment of steady-state voltage stability margins using the p–q–v curve," *Int. J. Electr. Power Energy Syst.*, vol. 32, no. 10, pp. 1091–1098, 2010.

[31] S. Kumar, B. Tyagi, V. Kumar, and S. Chohan, "Optimization of phasor measurement units placement under contingency using reliability of network components," *IEEE Trans. Instrum. Meas.*, vol. 69, no. 12, pp. 9893–9906, 2020.

[32] R.S. Wibowo, N. Yorino, M. Eghbal, Y. Zoka, and Y. Sasaki, "Facts devices allocation with control coordination considering congestion relief and voltage stability," *IEEE Trans. Power Syst.*, vol. 26, no. 4, pp. 2302–2310, 2011.

[33] A. Sode-Yome, N. Mithulananthan, and K.Y. Lee, "Comprehensive comparison of facts devices for exclusive loadability enhancement," *IEEJ Trans. Electr. Electron. Eng.*, vol. 8, no. 1, pp. 7–18, 2013.

[34] J.P. Roselyn, D. Devaraj, and S.S. Dash, "Multi-objective genetic algorithm for voltage stability enhancement using rescheduling and facts devices," *Ain Shams Eng. J.*, vol. 5, no. 3, pp. 789–801, 2014.

[35] B.B. Adetokun, C.M. Muriithi, and J.O. Ojo, "Voltage

stability assessment and enhancement of power grid with increasing wind energy penetration," *Int. J. Electr. Power Energy Syst.*, vol. 120, p. 105988, 2020.

[36] D.Q. Zhou, U.D. Annakkage, and A.D. Rajapakse, "Online monitoring of voltage stability margin using an artificial neural network," *IEEE Trans. Power Syst.*, vol. 25, no. 3, pp. 1566–1574, 2010.

[37] C. Zheng, V. Malbasa, and M. Kezunovic, "Regression tree for stability margin prediction using synchrophasor measurements," *IEEE Trans. Power Syst.*, vol. 28, no. 2, pp. 1978–1987, 2012.

[38] V. Ajjarapu and C. Christy, "The continuation power flow: a tool for steady state voltage stability analysis," *IEEE Trans. Power Syst.*, vol. 7, no. 1, pp. 416–423, 1992.

[39] M. Moghavvemi and F. Omar, "Technique for contingency monitoring and voltage collapse prediction," *IEE P-Gener. Transm. D.*, vol. 145, no. 6, pp. 634–640, 1998.

[40] P. Prabhakar and A. Kumar, "Voltage stability boundary and margin enhancement with facts and hvdc," *Int. J. Electr. Power Energy Syst.*, vol. 82, pp. 429–438, 2016.

[41] R. Sodhi, S. Srivastava, and S. Singh, "A simple scheme for wide area detection of impending voltage instability," *IEEE Trans. Smart Grid*, vol. 3, no. 2, pp. 818–827, 2012.

[42] Ieee 14-bus system, [Available: http://www.ee.washington.edu/research/pstca/pf14/pg_tca14bus.htm].

[43] M.A. Kamarposhti, M. Alinezhad, H. Lesani, and N. Talebi, "Comparison of svc, statcom, tcsc, and upfc controllers for static voltage stability evaluated by continuation power flow method," in *2008 IEEE Canada Electric Power Conference*, pp. 1–8, IEEE, 2008.

[44] Nrpg 246-bus data, [Available: https://www.iitk.ac.in/eeold/facilities/Research_labs/Power_System/NRPG-DATA.pdf].

[45] P. Sahu and M. Verma, "Optimal placement of pmus in power system network for voltage stability estimation under contingencies," in *2017 6th International Conference on Computer Applications In Electrical Engineering-Recent Advances (CERA)*, pp. 365–370, IEEE, 2017.